

## Photo and pH Stable, Highly-Luminescent Silicon Nanospheres and Their Bioconjugates for Immunofluorescent Cell Imaging

Yao He,<sup>†,‡,§</sup> Yuanyuan Su,<sup>§</sup> Xiaobao Yang,<sup>‡</sup> Zhenhui Kang,<sup>†,‡</sup> Tingting Xu,<sup>‡</sup>  
Ruiqin Zhang,<sup>‡</sup> Chunhai Fan,<sup>\*,§</sup> and Shuit-Tong Lee<sup>\*,‡</sup>

Functional Nano and Soft Materials Laboratory (FUNSOM), Soochow University, Suzhou, Jiangsu 215123, China, Center of Super-Diamond and Advanced Films (COSDAF) and Department of Physics and Materials Science, City University of Hong Kong, Hong Kong SAR, China, and Shanghai Institute of Applied Physics, Chinese Academy of Sciences, Shanghai 201800, China

Received November 10, 2008; E-mail: fchh@sinap.ac.cn; apannale@cityu.edu.hk

**Abstract:** We report a novel kind of oxidized silicon nanospheres (O-SiNSs), which simultaneously possess excellent aqueous dispersibility, high photoluminescent quantum yield (PLQY), ultra photostability, wide pH stability, and favorable biocompatibility. Significantly, the PLQY of the O-SiNSs is as high as 25%, and is stable under intense UV irradiation and in acidic-to-basic environments covering the pH range 2–12. To our best knowledge, it is the first example of water-dispersed silicon nanoparticles which possess both high PLQY and robust pH stability suitable for broad utility in bioapplications. Furthermore, the O-SiNSs are readily conjugated with antibody, and the resultant O-SiNSs/antibody bioconjugates are successfully applied in immunofluorescent cell imaging. The results show that the highly luminescent and stable O-SiNSs/antibody bioconjugates are promising fluorescent probes for wide-ranging bioapplications, such as long-term and real-time cellular labeling.

### 1. Introduction

The use of functional nanoparticles in biology is one of the fast moving and exciting interfaces of nanobiotechnology.<sup>1</sup> Particularly, fluorescent quantum dots (QDs) are appealing high-quality bioprobes for applications in diverse biological research because of their unique merits, such as size-tunable emission, strong fluorescence, and high photostability.<sup>2</sup> Notwithstanding, the well-studied II/VI QDs are handicapped by a potential toxicity problem due to release of heavy metal ions (e.g., Cd ions), which limits their biological and medical applications.<sup>3</sup> Consequently, the biocompatible and fluorescent silicon-based nanoparticles have recently attracted much interest, and extensive studies for applications as novel cellular probes.<sup>4,5</sup> For example, water-dispersed silicon QDs (SiQDs) capped with acrylic acid or allylamine were prepared for fluorescent cellular imaging,<sup>4a,b</sup> while micelle-encapsulated SiQDs were synthesized and used as luminescent cellular labels.<sup>4c</sup> We have recently

developed silicon nanospheres (SiNSs) with high photostability and strong luminescence for long-term cell imaging.<sup>5b</sup> Despite these advances, much work is still required for the development of a practical Si-based biomarker. Particularly, recent investigations reveal that SiQDs and SiNSs suffer from poor pH stability, although they are stable under normal conditions.<sup>4</sup> The meager pH stability severely hinders their broad applications in biology; e.g., conjugation of SiQDs or SiNSs with antibodies is technically difficult due to instability at neutral and alkaline pH environment. While micelle-encapsulated SiQDs preserve photoluminescent (PL) intensity in the pH range 2–10, their PL quantum yield (PLQY) is impractically low at only 2%.<sup>4c</sup> To date, there exists, to our best knowledge, no successful example of water-dispersed silicon nanoparticles which possess both high PLQY and robust pH stability suitable for broad utility in bioapplications.

Herein, we report a novel kind of water-dispersed oxidized SiNSs (O-SiNSs) prepared via thermal oxidation of the precursor SiNSs (see Supporting Information for experimental details). Significantly, the PLQY of the O-SiNSs is as high as 25% and is stable under high-power UV irradiation and in acidic-to-basic environments covering pHs 2–12. Furthermore, the O-SiNSs are readily conjugated with antibody, and the resultant O-SiNSs/antibody bioconjugates, acting as cellular probes, are successfully applied in immunofluorescent cell imaging.

<sup>†</sup> Soochow University.

<sup>‡</sup> City University of Hong Kong.

<sup>§</sup> Chinese Academy of Sciences.

- (1) (a) Won, J.; Kim, M.; Yi, Y. W.; Kim, Y. H.; Jung, N.; Kim, T. K. *Science* **2005**, *309*, 121–125. (b) Rothenfluh, D. A.; Bermudez, H.; O'Neil, C. P.; Hubbell, J. A. *Nat. Mater.* **2008**, *7*, 248–254.  
(2) Michalet, X.; Pinaud, F. F.; Bentolila, L. A.; Tsay, J. M.; Doose, S.; Li, J. J.; Sundaresan, G.; Wu, A. M.; Gambhir, S. S.; Weiss, S. *Science* **2005**, *307*, 538–544.  
(3) (a) Derfus, A. M.; Chan, W. C. W.; Bhatia, S. N. *Nano Lett.* **2004**, *4*, 11–18. (b) Kirchner, C.; Liedl, T.; Kudera, S.; Pellegrino, T.; Javier, A. M.; Gaub, H. E.; Stolzle, S.; Fertig, N.; Parak, W. J. *Nano Lett.* **2005**, *5*, 331–338. (c) Su, Y. Y.; He, Y.; Lu, H. T.; Sai, L. M.; Li, Q. N.; Li, W. X.; Wang, L. H.; Shen, P. P.; Huang, Q.; Fan, C. H. *Biomaterials* **2009**, *30*, 19–25.

- (4) (a) Li, Z. F.; Ruckenstein, E. *Nano Lett.* **2004**, *4*, 1463–1467. (b) Warner, J. H.; Hoshino, A.; Yamamoto, K.; Tilley, R. D. *Angew. Chem., Int. Ed.* **2005**, *44*, 4550–4554. (c) Erogbogbo, F.; Yong, K.; Roy, I.; Xu, G. X.; Prasad, P. N.; Swihart, M. T. *ACS Nano* **2008**, *2*, 873–878.

## 2. Experimental Section

**2.1. Materials and Devices.** Silicon wafer (phosphorus-doped (p-type),  $8\Omega$  sensitivity), hydrofluoric acid (HF), hydrogen peroxide, polyoxometalates (POMs), and acrylic acid (99%) were purchased from Sigma-Aldrich. Coumarin 540 (for fluorescence test) was purchased from Fluka. All chemicals were used as-received without additional purification. The human embryonic kidney cells 293 (HEK293) were cultured in Dulbecco's modified Eagle's medium (DMEM), supplemented with 10% heat-inactivated fetal bovine serum (FBS) and antibiotics (100  $\mu\text{g}/\text{mL}$  streptomycin and 100 U/mL penicillin) in the humidified atmosphere at 37  $^{\circ}\text{C}$  with 5%  $\text{CO}_2$  overnight.

The O-SiNSs were characterized by transmission electronic microscopy (TEM), high-resolution TEM (HRTEM), UV-vis absorption, photoluminescence (PL), Fourier transform infrared (FTIR) spectroscopy, inverted fluorescent microscopy, and laser scanning confocal fluorescent microscopy (LSCFM). TEM and HRTEM samples were prepared by dispersing the sample onto carbon-coated copper grids with the excess solvent evaporated. The TEM overview images were recorded using FEI/Philips Techal 12 BioTWIN TEM, while HRTEM images were obtained with a Philips CM 200 electron microscope operated at 200 kV. All optical measurements were performed at room temperature under ambient air conditions. UV-vis absorption spectra were recorded with a Shimadzu UV-3150 UV-vis-NIR spectrophotometer. PL measurements were performed using a Shimadzu RF-6301PC spectrofluorimeter. PLQY of the samples was estimated using Coumarin 540 in ethanol as a reference standard, which was freshly prepared to reduce the measurement error.<sup>6</sup> For Fourier-transform infrared (FTIR) measurements, KBr was pressed into a slice, onto which the SiNSs or O-SiNSs sample was dropped. The solvent in the sample was adequately evaporated by irradiation (>30 min) with a high-power incandescent lamp. FTIR spectra were taken on a Nicolet Avatar 370 FTIR spectrometer and cumulated 32 scans at a resolution of 4  $\text{cm}^{-1}$ . To characterize the  $\text{SiO}_2$  sample,  $\text{SiO}_2$  powders were pressed into a slice with KBr. Other manipulations were identical to those mentioned above. Inverted fluorescent microscopy (Olympus IX71) and LSCFM (Zeiss LSM510 ver 2.02) were used for fluorescent cellular imaging.

**2.2. Experimental Procedure.** **2.2.1. Synthesis of H-Terminated SiQDs, SiNSs, and O-SiNSs.** H-terminated SiQDs and SiNSs were synthesized following our previous reports.<sup>5</sup> Briefly, p-type Si wafer were cleaned in 20% hydrofluoric acid (HF) for 5 min to remove surface oxides and impurities. The electrolyte of the electrochemical etching process was prepared by mixing 60 mL of ethanol/HF solution (3:2) with 10 mL of  $\text{H}_2\text{O}_2$  (hydrogen peroxide 30%) and polyoxometalate (POM) as the catalyst. POM in ethanol ( $10^{-2}$  M) was used. The electrochemical system consisted of graphite as anode and the cleaned Si wafer as cathode. Graphite and Si wafer were put into the electrolyte and connected to the dc power supply by wires. A layer of n-hexane covered the electrolyte solution. The SiQDs were achieved in an etching process with a current density of 35  $\text{mA}/\text{cm}^2$  for 45–60 min, and were well dispersed in 100 mL ethanol solution by ultrasonic treatment. Afterward, the precipitates after ultrasonification were removed using a poly(tetrafluoroethylene) (PTFE) syringe filter (pore size 0.22  $\mu\text{m}$ ). Afterward, the purified SiQDs ethanol solution was utilized to synthesize SiNSs.

In a typical preparation of SiNSs, 10 mL of 98 wt % monomer acrylic acid solution was first introduced into the resultant SiQDs solution. The mixture was bubbled with  $\text{N}_2$  for 30 min to fully remove the dissolved oxygen, and then it was exposed to blue light

irradiation for 1 h under continuous magnetic stirring, allowing the acrylic acid (AAc) monomers to adequately react with the Si-H sites of the surface in the second step. Afterward, instead of blue light irradiation, UV irradiation was utilized to initiate the hydrosilylation reaction and the addition reaction of AAc in the third step. The SiNSs with sizes of about 120 nm were achieved with 2 h UV irradiation. The clear solution of SiNSs was further dialyzed in deionized water to completely remove the residual AAc monomers and free polymers. Such resultant SiNSs solution was diluted to 25 mL by the deionized water and utilized to synthesize O-SiNSs.

In a typical preparation of O-SiNSs, the precursor SiNSs solution was first bubbled with  $\text{O}_2$  for 30 min to guarantee full oxygen saturation of the solution. Afterward, the oxygen-saturated precursor SiNSs solution was heated to 80  $^{\circ}\text{C}$  for 1 h under continuous magnetic stirring in an open system, allowing the SiNSs to be adequately oxidized by oxygen under the elevated temperature condition. We point out that the whole process of oxidation by UV lamp was continually monitored, since the fluorescent color of O-SiNSs (green) was distinctively blue-shifted relative to that of SiNSs (orange) after UV irradiation, as described in the article. Consequently, the reaction was stopped when the fluorescent color of the solution was observed to turn green. Finally, O-SiNSs with sizes of about 35 nm were achieved. The resultant O-SiNSs solution was first filtered by using the PTFE syringe filter (pore size 0.22  $\mu\text{m}$ ) to fully remove the large-sized byproduct. The clear solution of O-SiNSs was further dialyzed in deionized water to completely remove the detached AAc monomers, free polymers, and SiQDs for photostability comparison, pH stability comparison, MTT measurement, protein conjugation, and fluorescent cellular imaging.

**2.2.2. Photostability Comparison of FITC, CdTe QDs, CdTe/CdS/ZnS QDs, SiNSs, and O-SiNSs.** CdTe QDs and CdTe/CdS/ZnS core-shell-shell QDs were synthesized according to previous reports.<sup>7</sup> To exclude the influences of residual reagents such as MPA,  $\text{Cd}^{2+}$ ,  $\text{Te}^{2-}$ , and  $\text{Zn}^{2+}$  in solution, the CdTe QDs and CdTe/CdS/ZnS QDs samples were subject to strict post-treatment before comparison. In detail, 2-propanol was added dropwise under stirring until the sample solution became slightly turbid. The turbid dispersion was continually stirred further for 15 min. The precipitate containing the first fraction of the sample was isolated from the supernatant by centrifugation. Another portion of 2-propanol was added dropwise to the supernatant to obtain the second precipitated fraction of the sample and so on. This procedure was repeated three times. The final CdTe QDs and CdTe/CdS/ZnS QDs precipitates were selected for photostability comparison. Moreover, the OD (optical density) values at the excitation wavelength of the solution samples of FITC dye, CdTe QDs, CdTe/CdS/ZnS QDs, SiNSs, and O-SiNSs were set to an identical value of 0.1. Finally, the five samples were irradiated for different time intervals using a 450 W xenon lamp of 365 nm.

**2.2.3. pH Stability Comparison of the SiQDs, SiNSs, and O-SiNSs.** The pH of the O-SiNSs solution was varied by dropwise addition of HCl or NaOH. The pH value was monitored by Seven Multi pH meter (Mettler Toledo); meanwhile, the corresponding PL intensity of the sample was recorded by the Shimadzu RF-6301PC spectrofluorimeter.

When SiQDs or SiNSs were used, the procedures were identical to those described above.

**2.2.4. MTT Assay of Cell Viability.** HEK293T cells (in DMEM Medium) were dispersed in 96-well plates (90  $\mu\text{L}$  in each well containing  $3 \times 10^4$  cells per well). A 10  $\mu\text{L}$  portion of the

- (5) (a) Kang, Z. H.; Tsang, C. H. A.; Zhang, Z. D.; Zhang, M. L.; Wong, N. B.; Zapien, J. A.; Shan, Y. Y.; Lee, S. T. *J. Am. Chem. Soc.* **2007**, *129*, 5326–5327. (b) He, Y.; Kang, Z. H.; Li, Q. S.; Tsang, C. H. A.; Fan, C. H.; Lee, S. T. *Angew. Chem., Int. Ed.* **2009**, *48*, 128–132. (6) (a) Grosby, G. A.; Demas, J. N. *J. Phys. Chem.* **1971**, *75*, 991–1024. (b) Qu, L.; Peng, X. *J. Am. Chem. Soc.* **2002**, *124*, 2049–2055.

- (7) (a) He, Y.; Lu, H. T.; Sai, L. M.; Lai, W. Y.; Fan, Q. L.; Wang, L. H.; Huang, W. *J. Phys. Chem. B* **2006**, *110*, 13352–13356. (b) He, Y.; Lu, H. T.; Sai, L. M.; Lai, W. Y.; Fan, Q. L.; Wang, L. H.; Huang, W. *J. Phys. Chem. B* **2006**, *110*, 13370–13374. (c) He, Y.; Sai, L. M.; Lu, H. T.; Hu, M.; Lai, W. Y.; Fan, Q. L.; Wang, L. H.; Huang, W. *Chem. Mater.* **2007**, *19*, 359–365. (d) He, Y.; Lu, H. T.; Sai, L. M.; Su, Y. Y.; Hu, M.; Fan, C. H.; Huang, W.; Wang, L. H. *Adv. Mater.* **2008**, *20*, 3416–3421.



O-SiNSs solution with the same concentration as that used in the following cellular imaging was added to each well. Incubation was carried out for 2, 12, 24, and 48 h, in a humidified atmosphere at 37 °C with 5% CO<sub>2</sub>. The cytotoxicity of the O-SiNSs was evaluated by the MTT (3-(4,5-dimethylthiazol-2-yl)-2,5-diphenyltetrazolium bromide) assay (thiazolyl blue tetrazolium bromide (M5655); Sigma). The assay was based on the accumulation of dark blue formazan crystals inside living cells after their exposure to MTT. The destruction of cell membranes by the addition of sodium dodecylsulfate (SDS) resulted in the liberation and solubilization of the crystals. The number of viable cells was thus directly proportional to the level of the initial formazan product created. The formazan concentration was finally quantified using a spectrophotometer by measuring the absorbance at 570 nm (ELISA reader). A linear relationship between cell number and optical density was established, thus allowing an accurate quantification of changes in the rate of cell proliferation.

**2.2.5. Preparation of the O-SiNSs/Antibody Conjugates.** The carboxylic acid groups of O-SiNSs readily reacted with the amino groups of the protein by using *N*-(3-dimethylaminopropyl)-*N*-ethylcarbodiimide hydrochloride (EDC) and *N*-hydroxysuccinimide (NHS) as zero-length cross-linkers.<sup>8</sup> A 20  $\mu$ L portion of EDC (6.4 mg/mL in H<sub>2</sub>O) and 17  $\mu$ L NHS (7.7 mg/mL in H<sub>2</sub>O) were first added to 50  $\mu$ L O-SiNSs (in 150 mM PBS, pH = 7.4). The mixed solution was then incubated at 25 °C for 15 min to fully activate the O-SiNSs. Afterward, 30  $\mu$ L goat antimouse IgG (4 mg/mL) in PBS buffer was added to the activated O-SiNSs. The resultant solution was incubated for 2 h at 25 °C under shaking in dark and then kept overnight at 4 °C. No obvious precipitation was observed after this conjugation reaction. The isourea byproduct and residual reagent (e.g., IgG with molecular weight of  $\sim$ 168 kDa) were filtrated in the lower phase by using 300 kDa Nanosep centrifugal devices through centrifugation at 5000 rpm for 15 min. The upper phase containing the O-SiNSs/IgG conjugates was diluted by 300  $\mu$ L PBS buffer. The conjugates solution was further centrifuged (5000 rpm, 15 min) and diluted by 100  $\mu$ L PBS buffer for three times to completely remove the impurities. Finally, the resultant conjugates were stored at 4 °C in the dark for immunofluorescent cellular imaging.

**2.2.6. Fluorescent Labeling Fixed HEK293 Cells Using the O-SiNSs/Antibody Conjugates.** HEK293T human kidney cells were stained with the O-SiNSs/antibody conjugates for the bioimaging experiment. The HEK293T cells were cultured in Dulbecco's modification of Eagles media (DMEM), supplemented with 10% heat-inactivated fetal bovine serum (FBS) and antibiotics (100  $\mu$ g/mL streptomycin and 100 U/mL penicillin) in a humidified atmosphere at 37 °C with 5% CO<sub>2</sub>. Briefly, 5000 HEK293T cells in 2 mL culture medium were fixed using 400  $\mu$ L ethanol (75%) and washed with PBS for three times. Afterward, the cells were incubated for 30 min at 25 °C in 1% BSA in PBS. The fixed cells were further incubated with the as-prepared O-SiNSs/antibody bioconjugates for 15 min at 25 °C, and then washed with PBS for three times to remove excess unbound bioconjugates. The stained cells were imaged using LSCFM.

**2.2.7. Two-Color Staining Fixed HEK293 Cells Using the O-SiNSs/Antibody Conjugates and Hoechst.** The human embryonic kidney cells line 293 (HEK293) were cultured in Dulbecco's modified Eagle's medium (DMEM), supplemented with 10% heat-inactivated fetal bovine serum (FBS) and antibiotics (100  $\mu$ g/mL streptomycin and 100 U/mL penicillin) in the humidified atmosphere at 37 °C with 5% CO<sub>2</sub> overnight. The cells were first washed twice using warmed PBS (35 °C) and then were fixed with paraformaldehyde (200  $\mu$ L, 3%) and saccharose (200  $\mu$ L, 3%) for 20 min, and then washed with PBS (150 mM, pH 7.3) and glycine (100 mM) mixed solution three times. After washing with PBS (150 mM, pH

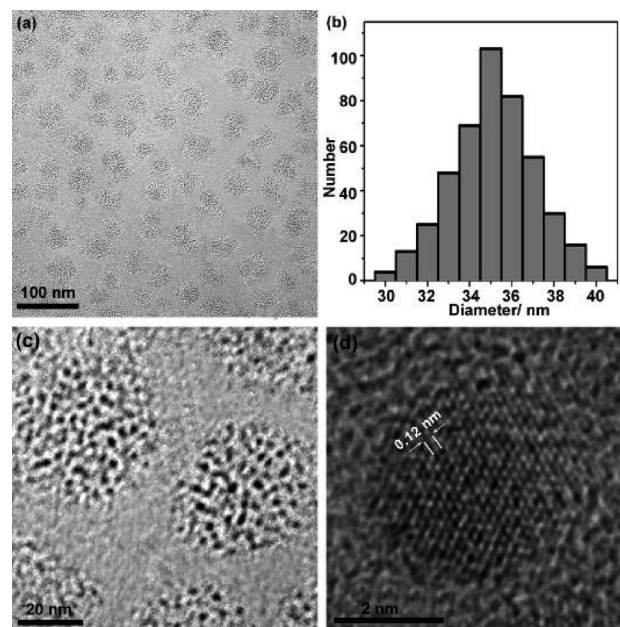


**Figure 1.** TEM overview image (a), the size distribution (b), and enlarged TEM image (c) of O-SiNSs. HRTEM image of a single SiQD inside the O-SiNS (d).

7.3) and glycine (100 mM) mixed solution three times, the cells were blocked with P-block for 40 min. Thereafter, the primary antibodies (mouse antiactin antibodies, 1:300 diluted by P-block) were incubated with HEK293 cells for 60 min. The cells were further incubated with the O-SiNSs/IgG bioconjugates (secondary antibodies) for 60 min, and then washed with PBS three times and Milli-Q water twice. Afterward, the cell nuclei were stained with Hoechst 33258 (3  $\mu$ g/mL) for 5 min and washed with Milli-Q water twice. The resultant cells were imaged by using the inverted fluorescent microscopy.

### 3. Results and Discussion

Figure 1 displays the TEM/HRTEM images, and size distributions of the prepared O-SiNSs. As shown in Figure 1a, the O-SiNSs possess a spherical structure and good dispersity. The size distribution measured from over 350 nanospheres yields an average size of  $35.1 \pm 5.4$  nm, and polydispersity of 16.5% (Figure 1b). The enlarged TEM image shows  $\sim$ 100 SiQDs in one nanosphere (Figure 1c). The O-SiNSs are reduced in size compared to the precursor SiNSs (Figure 1 in Supporting Information). A reasonable explanation is that the SiQDs in the peripheral region of the precursor SiNSs are prone to be detached under high-temperature and long-time oxidation.<sup>9</sup> Importantly, the SiQDs inside the O-SiNSs preserve the original Si properties because they display characteristic Si crystal lattice and high crystallinity (Figure 1d).

To show the changes of the dominant chemical bonding that occurred upon oxidation, the FTIR spectra of the SiNSs (blue line) and O-SiNSs (red line) were measured and compared in Figure 2. Significantly, both spectra show distinctive absorbance peaks at  $1187\text{ cm}^{-1}$ , which are attributed to the vibration stretch of Si–O bonding.<sup>4b,10</sup> The slightly blue-shifted peak position relative to that of the referenced Si–O bond (black line,  $1100$

(8) (a) So, M. K.; Loening, A. M.; Gambhir, S. S.; Rao, J. H. *Nat. Proto.* **2006**, *1*, 1160–1164. (b) Clapp, A. R.; Goldman, E. R.; Mattoussi, H. *Nat. Proto.* **2006**, *1*, 1258–1267.

(9) Higgins, K. J.; Jung, H.; Kittelson, D. B.; Roberts, J. T.; Zachariah, M. R. *J. Phys. Chem. A* **2002**, *106*, 96–103.

(10) (a) Kato, Y.; Yamazaki, H.; Tomozawa, M. *J. Am. Chem. Soc.* **2001**, *84*, 2111–2116. (b) Bansal, V.; Ahmad, A.; Sastry, M. *J. Am. Chem. Soc.* **2006**, *128*, 14059–14066.

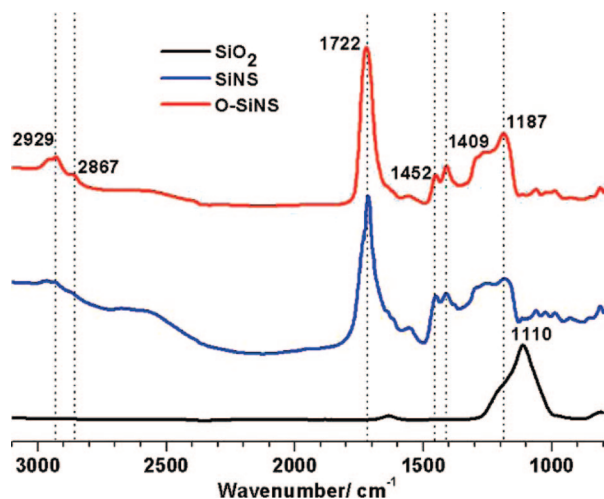


**Figure 2.** FTIR spectra of SiNSs and O-SiNSs. The FTIR spectrum of SiO<sub>2</sub> is also presented for reference.

cm<sup>-1</sup>) is probably due to the different structural relaxation of the SiNSs/O-SiNSs and SiO<sub>2</sub> samples.<sup>10a</sup> Additionally, compared to that of the SiNSs, the sharper and stronger Si–O peak of O-SiNSs implies that more Si–O bonds are formed by thermal oxidation.<sup>10b,11</sup> Besides, the absorbances in the ranges of 1409–1452 and 2867–2969 cm<sup>-1</sup>, which are assigned to the deformation and stretch vibration of O–H bond,<sup>12</sup> are also changed to some extent. We thus conclude thermal oxidation to be the dominant factor leading to the differences of the oxygen-related chemical bonds (e.g., Si–O and O–H bonds) between the SiNSs and O-SiNSs. It is worthwhile to point out that the strong peak at 1772 cm<sup>-1</sup>, which is attributed to the C=O stretching vibration in SiNSs and O-SiNSs spectra, indicates the resultant nanospheres have a large amount of carboxylic group.<sup>13</sup> Notably, in comparison to the clear Si–H stretching peak (900 cm<sup>-1</sup>) in the precursor SiQDs,<sup>5a</sup> the corresponding peak disappeared in the spectra of the nanospheres. It provides a convincing demonstration of the full removal of Si–H bonds in the prepared nanospheres.<sup>11</sup>

Figure 3a displays a clearly resolved absorption peak of the first electronic transition and a symmetrical photoluminescence peak, indicating the good optical properties of the prepared O-SiNSs. More importantly, compared to that of the free-standing SiQDs (~3%) and SiNSs (~17%), the PLQY of the O-SiNSs is greatly enhanced to 25%. Interestingly, the PL peak of the O-SiNSs is remarkably blue-shifted by ~50 nm (Figure 3b) from that of the SiQDs and SiNSs. Our theoretical calculation suggests the PLQY enhancement and the blue-shift in PL are due to the new electronic gap states and a larger HOMO–LUMO energy gap of the O-SiNSs (see Figure 2 in Supporting Information and corresponding theoretical discussion). Significantly, the PL of the O-SiNSs exhibits excellent photostability and pH stability. Figure 3c shows that the PL intensity of FITC (one kind of traditional dyes) quickly vanished in 5 min due to severe photobleaching. Although II/VI QDs

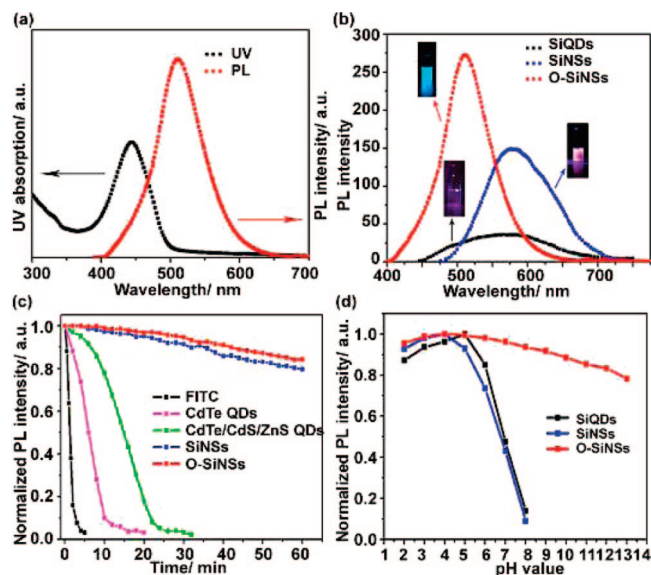


**Figure 3.** Absorption and PL spectra of O-SiNSs (a). PL spectra of SiQDs, SiNSs, and O-SiNSs sample with an identical optical density of 0.10 (b). The insets display the corresponding optical micrographs of the sample under UV irradiation. Photostability comparison of FITC, II/VI QDs, SiNSs, and O-SiNSs (c). pH stability comparison of SiQDs, SiNSs, and O-SiNSs (d).

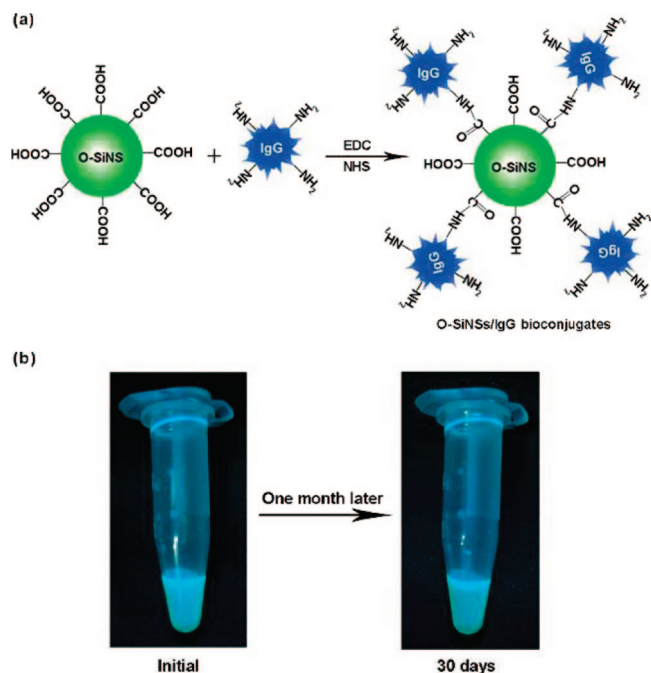


**Figure 4.** Schematic illustration of O-SiNSs conjugating with goat-antimouse IgG (a). The carboxylic acid groups of O-SiNSs readily reacted with the amino groups of IgG by using EDC and NHS as zero-length cross-linkers (figure is not to scale). Optical micrographs of the prepared O-SiNSs/IgG bioconjugates under UV (365 nm) irradiation (b). The prepared O-SiNSs/IgG bioconjugates display bright fluorescence (left), and preserve stable fluorescent intensity for over 1 month (right).

- (11) He, J. L.; Ba, Y.; Ratcliffe, C. I.; Ripmeester, J. A.; Klug, D. D.; Tse, J. S.; Preston, K. F. *J. Am. Chem. Soc.* **1998**, *120*, 10697–10705.
- (12) (a) Jacobsen, S. D.; Demouchy, S.; Frost, D. J.; Ballaran, T. B.; Kung, J. *Am. Mineral.* **2005**, *90*, 61–70. (b) Biemmi, E.; Bein, T. *Langmuir* **2008**, *24*, 11196–11202.
- (13) (a) Jun, Y.; Zhu, X. Y. *J. Am. Chem. Soc.* **2004**, *126*, 13224–13225. (b) Du, X. Z.; Miao, W. G.; Liang, Y. Q. *J. Phys. Chem. B* **2005**, *109*, 7428–7434. (c) Kaake, L. G.; Zou, Y.; Panzer, M. J.; Frisbie, C. D.; Zhu, X. Y. *J. Am. Chem. Soc.* **2007**, *129*, 7824–7830.

are known to be much more photostable, the PL of CdTe QDs and CdTe/CdS/ZnS core–shell–shell QDs nevertheless becomes negligible in 15 and 30 min, respectively, under high-power UV irradiation (CdTe/CdS/ZnS QDs are more photostable than CdTe QDs due to protection by the double shells).<sup>7</sup> In striking contrast, both SiNSs and O-SiNSs possess remarkably robust photostability; their PL maintains >80% of the original



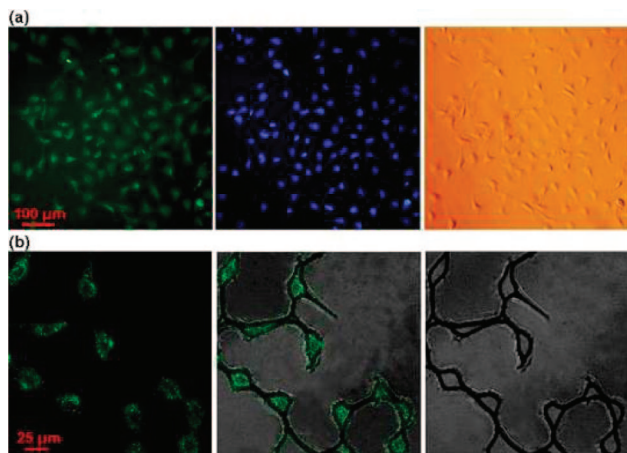


**Figure 5.** Dual-color cellular imaging photos (a). The HEK293 cells are distinctively labeled by the bioconjugates (left panel, green) and Hoechst (middle panel, blue); the right panel shows a bright field image. The bioconjugates fluorescently label the cells incubated with monoclonal mouse antiactin antibody (b). Left panel shows 488 nm excitation, middle panel shows superposition of fluorescence and transillumination images, and right panel shows bright field image.

intensity even after 60-min irradiation. As previously reported, the protection from the polymer shell and the unique PL properties of SiQDs are regarded as two dominant factors of the excellent photostability.<sup>5b,14</sup> Nevertheless, both the PL of SiQDs and SiNSs almost completely disappeared at pH value  $>7.0$ , as shown in Figure 3d. Remarkably, in striking contrast, the O-SiNSs preserve high photostability and strong photoluminescence in the wide pH range 2–12. Such great improvement of pH stability is attributable to the distinctive surface properties of the O-SiNSs, similar to those in the reported micelle-encapsulated SiQDs.<sup>4c</sup> Note that robust pH stability is critically important for various bioapplications. Of further importance is that the O-SiNSs can be readily conjugated with proteins (e.g., goat-antimouse IgG) in PBS buffer (pH  $\sim 7.4$ ), and that the prepared O-SiNSs/protein bioconjugates maintain very bright and stable fluorescence for over 1 month (Figure 4).

(14) Godefroo, S.; Hayne, M.; Jivanescu, M.; Stesmans, A.; Zacharias, M.; Lebedev, O. I.; Tendeloo, G.; Moshchalkov, V. V. *Nat. Nanotechnol.* **2008**, 3, 174–178.

The O-SiNSs/protein bioconjugates are successfully applied in immunofluorescent cell imaging. Figure 5a shows that HEK293T cells are distinctively double-color labeled by the bioconjugates and a nuclear dye Hoechst (a commercially available organic dye). To our best knowledge, this is the first example of silicon-based double-color cell imaging up till now, demonstrating that cellular multilabeling and multianalysis can be realized by the highly fluorescent and stable O-SiNSs/protein bioconjugates. Besides, the picture imaged by laser scanning confocal fluorescent microscope (LSCFM) shows that the PL of the bioconjugates-labeled HEK293T cells is very bright and clearly resolved spectrally (Figure 5b). In addition, MTT assays reveal that the O-SiNSs possess favorable biocompatibility due to the noncytotoxicity of silicon, in well accord with previous reports.<sup>4,5</sup>

#### 4. Conclusions

To summarize, we introduce a new kind of water-dispersed O-SiNSs, which possess high PLQY, ultra photostability, wide pH stability, and favorable biocompatibility. Significantly, the O-SiNSs can be readily conjugated with antibody, and the resultant O-SiNSs/antibody bioconjugates are successfully applied in immunofluorescent cell imaging. The results show that the highly luminescent and stable O-SiNSs/antibody bioconjugates are promising novel fluorescent biological probes for various bioapplications, such as long-term and real-time cellular labeling.

**Acknowledgment.** This work was supported by the Research Grants Council of Hong Kong (CityU 101608), Innovation & Technology Commission (ITS/029/08), 863 project (2006AA03Z302), NSFC (20725516), and the National Basic Research Program of China (2006CB93000, 2007CB936000). The authors thank Professor L. H. Wang for the fruitful discussion; Dr. C. W. L. Michael, and Dr. X. Fan for TEM/HRTEM characterizations; Dr. S. J. He and Dr. B. Deng for FTIR measurement; and Dr. C. H. A. Tsang, Dr. M. Hu, and Dr. H. T. Lu for providing SiQDs, CdTe QDs, and CdTe/CdS/ZnS QDs.

**Supporting Information Available:** Theoretical calculation and discussion, and supporting Figures 1 and 2. This information is available free of charge via the Internet at <http://pubs.acs.org>.

JA808827G